Middle-East Journal of Scientific Research 9 (2): 177-183, 2011
ISSN 1990-9233

Performance Comparison of R407c and R22 in Off-Design Point Using Wilson-Plot Method

Saber Zali, Reza hashemi and Mohammad naggashzadagan

Khalkhal Branch, Islamic Azad University, Khalkhal, Iran

Abstract: In this study, we modeled the thermodynamic properties of refrigerants, condenser and evaporator secondary fluid using artificial neural network. Benefits of this method are reducing complicated computation and not using state equations. Then, we used Wilson-Plot method to compare performance of refrigeration cycle with R22 and R407C refrigerants. Then we studied the effect of various parameters on cycle performance. Finally, we investigated benefits and disadvantages of R407C as an alternative for replacing with R22 in refrigeration cycle.

Key words: Refrigeration · Off-design · Wilson-Plot · Neural network · Performance

INTRODUCTION

Replacing chlorofluorocarbons in refrigeration industry is considered as an important problem because of environment depletion. On this way effort of environment fans caused international pressure for replacing of R22 and selecting a suitable refrigerant in compression refrigeration system. R407C is a mixture refrigerant and its thermodynamic and physical properties are like as R22. This refrigerant has been introduced as an alternative for R22 with zero ozone depletion potential and less greenhouse warming potential than R22. In practice, refrigeration cycle works in on-design or off-design point. If all of the conditions which we considered in the design be established when working system, it has to be said that the system works in design point. If usual condition such as environment temperature, secondary fluid mass rate, frost increasing around the evaporator coils, defrost time and refrigerant charge have been unsuitable, in this condition we are far from design point. In this condition we say that refrigeration cycle works in off-design point.

In this study, we used Wilson-plot method for investigating compression refrigeration cycle. Wilson-plot method uses the measurement of total heat transfer coefficient in refrigerant various mass rates for calculating convection heat transfer coefficient [1].

Many studies have been done in the field of the Wilson-Plot application for determining heat exchanger convection coefficient. Samuel M. Sami and *et al*. along with experimental study on the properties of diphase stream of R-502 refrigerant, proposed a method for prospect of the heat transfer parameters such as mean heat transfer and pressure drop [2]. Fan Pin Ching and Ru Yang have done an experimental study on the heat transfer of periodic tubes. They used the Wilson-Plot method for calculating heat transfer coefficient [3]. John W. Rose investigated the restriction of accruing heat transfer coefficient using Wilson-plot method. They concluded that in use of Wilson-plot method in saturation state should be accurate because of uncertainty in heat transfer coefficient. Jose Fernandez-Seara and *et al*. studied Wilson-plot method and the changes which were done for improvement of it. Finally they expanded this method for using in multitude problems [5]. Fernando Primal and *et al*. survived a shell and tube heat exchanger which was used in refrigeration system for minimizing the charge of system. They used the Wilson-Plot method for calculating heat transfer [6]. H. Shokohmand and *et al*. studied the coil tube heat exchanger using Wilson-Plot method experimentally by considering diverse situation of stream [7]. Ya Xiaowen and W. L. Lee studied helical heat exchanger for inner recycling of ventilation system which is cool with water. They used Wilson-plot method for calculating heat transfer coefficient [8]. P. Balachander and Tusha Rani studied the numerical model of fin and tube condenser with R22 and R407C refrigerants. In this study, the effect of environment temperature variation on pressure drop, condenser heat transfer rate, effect of condenser temperature variation on the pressure drop and the rate of heat transfer were investigated [9].

Corresponding Author: Saber Zali, Khalkhal Branch, Islamic Azad University, Khalkhal, Iran.

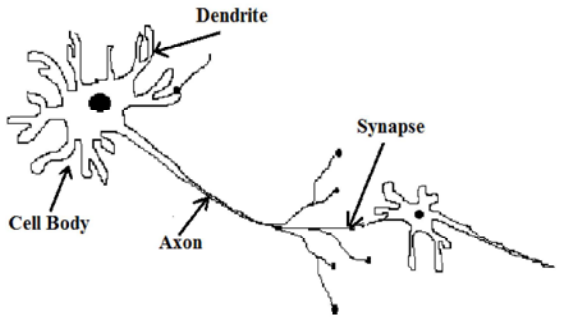

Fig. 1: A biological neuron [10]

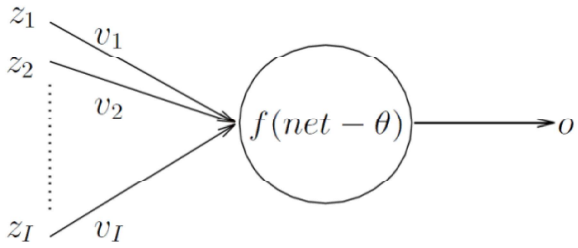

Fig. 2: An artificial neuron [10].

As we saw, Wilson plot method was used as a successful method to accruing heat transfer coefficient. Therefore, in this paper we used Wilson-plot method for analyzing refrigeration system by studying done work in this field. In this study, we used Artificial Neural Network (ANN) for calculating thermodynamic properties of refrigerant and secondary fluid.

Artificial Neural Network (ANN): ANN is a system which was inspired from human beings brain. The main part of biological neural system is neural cell which is called Neuron. As we see in fig (1) neuron connects to the other cell's dendrites by synapses. Signals transfer to the cell body by dendrites then transfer to axon. Neuron can amplify or castrate the signal. Artificial neuron model has been inspired from actual neuron.

An artificial neuron (AN) is a nonlinear mapping from R^I to [0 1] or [-1 1]. An artificial neuron receives a vector with *I* input signals which these inputs are the output of the other neurons or the signals from environment. For each of inputs (Z_i) a weight is considered which amplify or castrate the input. AN multiply inputs by weight then sums all of them. It uses an activation function (F_{AN}) for calculating the output. The power of output is affected by threshold quantity. Fig (2) shows an AN model [10].

$$Z = (z_1, z_2, ..., z_i) \quad (1)$$

$$Net = \sum_{i=1}^{I} z_i v_i \quad (2)$$

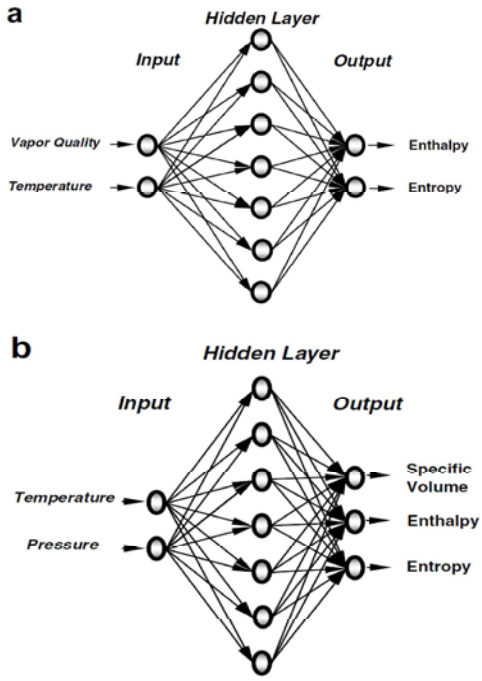

Fig. 3: A model of artificial neural network for (a) saturation (b) superheat or sub cooling condition

An ANN is a layer of ANs. As we see in fig (3) an ANN has input, hidden and output layers. These layers construct an ANN as shown in fig (3).

The problem is the method of selecting weights (v_i) and threshold quantities. For this problem we can use the training of ANN. Neurons select the best quantities for v_i and è using the defined inputs and outputs in training process. The training determines that how regulate these parameters to have minimum error. Error is the difference between network output and real quantity of output.

As shown in fig (3), for determining thermodynamic properties in saturation zone, we use temperature and quality of vapor as input and output is enthalpy and entropy. In superheat and sub cooling zone we use temperature and pressure as input too. Therefore, ANN can determine special volume, enthalpy and entropy.

It is important how to determine the number of layers and number of neuron's hidden layers to have acceptable accuracy. For selecting parameters we use trial and error method to have best output. In this study, we used tangent hyperbolic function for input layer and we used linear function for output and hidden layers.

Wilson-Plot Method: Wilson- plot method is used to calculate convection heat transfer coefficient by measuring total heat transfer. Wilson considered that

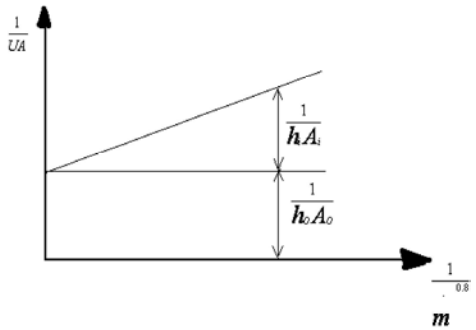

Fig. 4: Wilson-plot graph

the heat transfer coefficient is the linear function of secondary fluid heat transfer coefficient [11].

The total heat transfer resistance $(\frac{1}{UA})$ is equal to the sum of heat transfer resistance in both side of tube wall (secondary fluid and refrigerant) and conduction resistance of the Wall.

$$\frac{1}{U.A} = \frac{1}{(h.A)} + \frac{\delta}{KA_m} + \frac{1}{(h.A)_o} \tag{3}$$

In Equation (3) δ is neglect in compression with k, therefore we withdraw from $\frac{\delta}{kA_m}$. Therefore we have:

$$\frac{1}{U.A} = \frac{1}{h_i A_i} + \frac{1}{h_o A_o} \tag{4}$$

In equation (4) the refrigerant convection heat transfer coefficient (h_o) obtained from the design point equations and its quantity in design point is considered constant. h_i is obtained from secondary fluid mass rate. Therefore the total heat transfer coefficient is the function of h_i. If secondary fluid is flown in tube, heat transfer coefficient can be determined from equation (5) [12].

$$Nu = \frac{h.D}{K} = 0.023 \mathrm{Re}^{n}.\mathrm{Pr}^{m} \tag{5}$$

Prantdel number is neglected because of negligible variation in domain of temperature variation. Therefore:

$$h = C_2 \frac{K}{D}(\frac{\rho.u.D}{\mu}) \tag{6}$$

By replacing the mass rate of secondary fluid in equation (6) we will have:

$$\dot{m} = \rho.u.n.A \tag{7}$$

$$h = C.\dot{m}^{n} \tag{8}$$

If we replace equation (8) in equation (4) we will have:

$$\frac{1}{UA} = \frac{1}{h = C.\dot{m}^{n} A_i} + \frac{1}{h_o A_o} \tag{9}$$

If we write the equation (9) at A_0 and consider constant quantity for h_0 we will have:

$$\frac{1}{U} = \frac{1}{C.\dot{m}^{n}} + Cons\tan t = \frac{1}{h_1} Cons\tan t \tag{10}$$

If we plot $\frac{1}{UA}$ VS $\frac{1}{m^n}$, Wilson-plot graph will be as following.

Modeling of Compression Refrigeration Cycle in off Design Point: In this section we want to model refrigeration cycle using thermodynamic and heat transfer equations in off-design point. In fact we want to see the effect of secondary mass rate flow variation on performance coefficient, condenser temperature, refrigeration capacity and etc.

For this purpose we consider secondary fluid mass rate, area of condenser and evaporator as input for model. According to Wilson-plot method by variation of mass rate the variation of refrigeration convection heat transfer coefficient in condenser and evaporator will be negligible and we can consider constant. The quantity of these parameters is used from design point quantities.

Using equation (11) we can obtain the heat transfer coefficient of water in condenser and evaporator [13].

$$NU = \frac{hd}{K} = 0.023\ \mathrm{Re}^{m}\mathrm{Pr}^{n} \tag{11}$$

"m" and "n" are constant which are determined for condenser and evaporator according to table(1).

Now we can obtain the total heat transfer coefficient of surface. We can calculate the heat transfer of evaporator and condenser using equation (12).

$$Q = UA\Delta T_m \tag{12}$$

$$\mathrm{LMTD} = \frac{\Delta T_1 - \Delta T_2}{In\left(\frac{\Delta T_1}{\Delta T_2}\right)} \tag{13}$$

Table 1: Condenser and evaporator constants for heat transfer coefficient

	m	N
Evaporator	0.6	0.3
Condenser	0.8	0.4

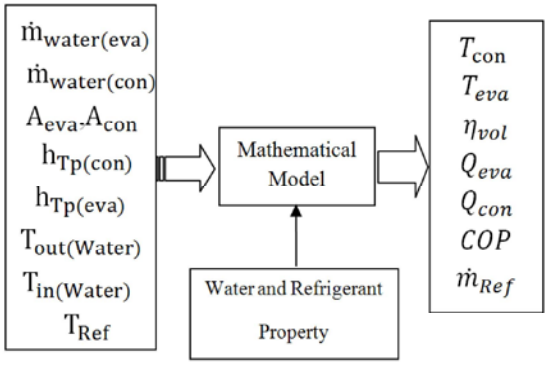

Fig. 5: Compression refrigeration cycle model flowchart

ΔT_1 and ΔT_2 are the fluid temperature difference between input and output of evaporator and condenser. We can obtain heat transfer using the variation of enthalpy and mass rate of refrigerant.

$$Q = \dot{m}_{Ref} \Delta h \tag{14}$$

Because the sub cooling and superheat zone in evaporator and condenser is small, therefore we can suppose that the temperature of refrigerant is constant in input and output and we can use the saturation temperature. Now using trial and error method and considering equal the equation of (12) and (14) we can obtain evaporator and condenser temperature and mass rate of refrigerant. Consequently, we can obtain COP using equation (15).

$$COP = \frac{Q_{av}}{W_{com}} \tag{15}$$

Volume efficiency of compressor can be calculated using equation (16).

$$\eta_{vol} = 1 + \frac{V_c}{V_s} - \frac{V_c}{V_s}\left(\frac{P_c}{P_e}\right)^{\frac{1}{n}} \tag{16}$$

Fig. 5 Shows the flowchart of the above model.

RESULTS AND DISCUSSION

In this section the results for this model are shown and therefore the performance of cycle, condenser and evaporator temperature are compared for R22 and R407C refrigerants by variation of secondary fluid mass rate in off-design point.

Condenser Water Mass Rate Effect on Condenser and Evaporator Temperature: Fig (6) and fig (7) show respectively the variation of condenser and evaporator temperature VS water mass rate in condenser.

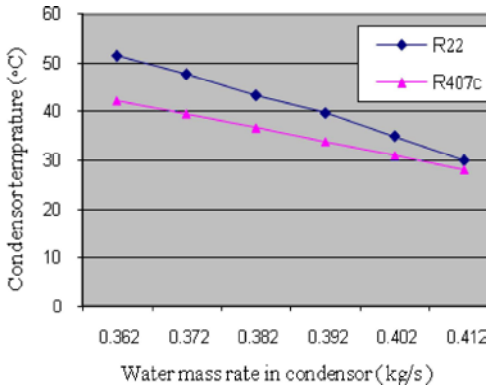

Fig. 6: Condenser water mass rate effect on condenser temperature

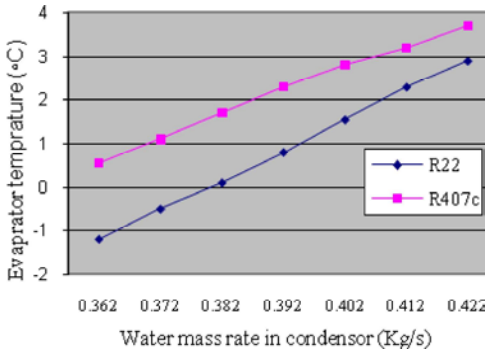

Fig. 7: Condenser water mass rate effect on evaporator temperature

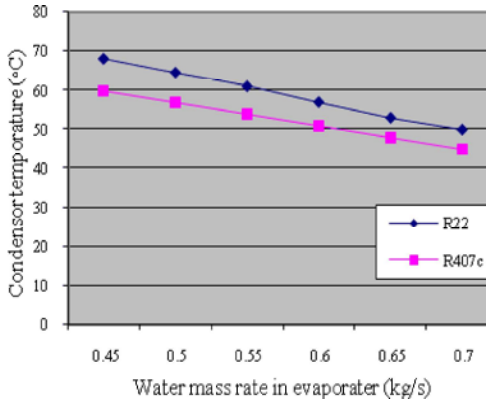

Fig. 8: Evaporator water mass rate effect on condenser temperature

Fig (6) shows that the condenser with R407C has ever less temperature than R22. By increasing water mass rate in condenser its temperature reduces.

Fig (7) shows that evaporator with R407C refrigerant has higher temperature than R22. By increasing water mass rate in condenser its temperature increases and by decreasing water mass rate its temperature decreases.

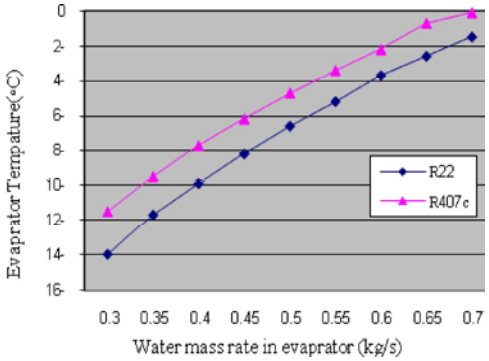

Fig. 9: Evaporator water mass rate effect on evaporator temperature

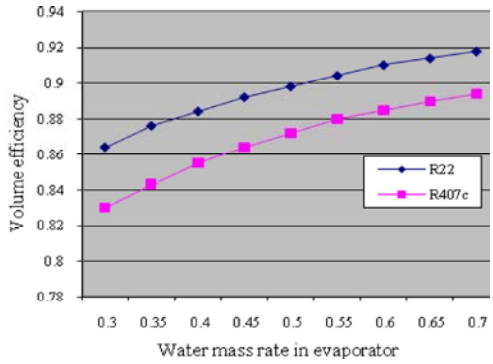

Fig. 11: Condenser water mass rate variation effect on compressor volume efficiency

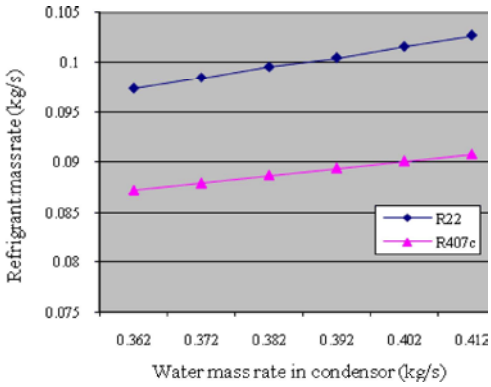

Fig. 10: Condenser water mass rate variation effect on compressor volume efficiency

Fig. 12: Condenser water mass rate effect on the refrigerant mass rate

Evaporator Water Mass Rate Effect on Condenser and Evaporator Temperature: Fig (8) and (9) show respectively evaporator and condenser temperature variation VS water mass rate variation in evaporator. Fig (8) shows that evaporator with R407C refrigerant has always more temperature than R22. By increasing mass rate in evaporator its temperature increases. Fig (9) shows that condenser with R407C refrigeration has always less temperature than R22. By increasing water mass rate evaporator, condenser temperature decreases.

The Effect of Water Mass Rate Variation in Condenser and Evaporator on Volume Efficiency: Fig (10) and (11) respectively show variation of volume efficiency of compression refrigeration cycle VS water mass rate in condenser and evaporator. In these figures R407C refrigerant has always less volume efficiency than R22. It is noticeable that in Fig(10) by increasing water mass rate in condenser, the volume efficiency increases and by decreasing water mass rate the volume efficiency decreases and difference between volume efficiency of R22 and R407C is 0.5% to 2% for mass rate of 0.362 kg/s to 0.412 kg/s. Fig (11) shows that by increasing water mass rate the volume efficiency decreases and the difference between volume efficiency of R22 and R407C is 2.5% to 5% for mass rate of the 0.3kg/s to 0.7 kg/s.

Condenser and Evaporator Water Mass Rate Effect on the Refrigerant Mass Rate: Fig (12) and (13) respectively show refrigeration mass rate variation VS water mass rate in condenser and evaporator. These figures show that R407C has less water mass rate than the R22.

Fig (12) shows that by increasing water mass rate in condenser, refrigerant mass rate increases. The difference between mass rate of R22 and R407C is 11% to 12% for water mass rate of 0.362 kg/s to 0.412 kg/s.

Fig (13) shows that by increasing water mass rate in evaporator, refrigerant mass rate increases. The Difference between mass rate of R22 and R407C is 8% to 9% for water mass rate of 0.3 kg/s to 0.7 kg/s.

Evaporator and Condenser Water Mass Rate Effect on Evaporator Refrigeration Capacity: Fig (14) and (15) respectively show refrigeration capacity VS water mass rate in evaporator and condenser. These figures show that always R407C has less refrigeration capacity than

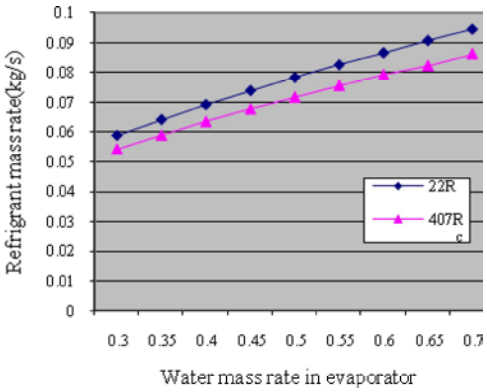

Fig. 13: Evaporator water mass rate effect on the refrigerant mass rate

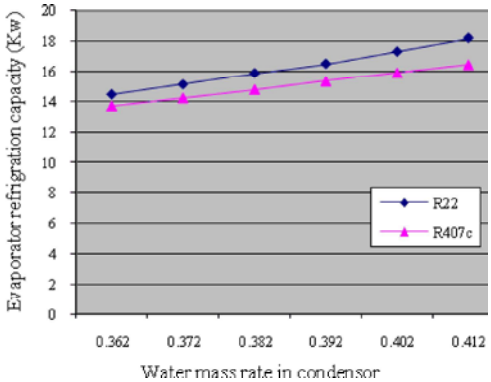

Fig. 14: Condenser water mass rate effect on evaporator refrigeration capacity

R22. Fig (14) shows that by increasing water mass rate in condenser refrigeration, capacity. Refrigeration capacity difference between R22 and R407C is 5% to 9% for water mass rate from 0.362 kg/s to 0.412 kg/s. It is noticeable that in fig (15) by increasing water mass rate in evaporator, refrigeration capacity increases. Difference between refrigeration capacity for R22 and R407C is about 11% for water mass rate of 0.3 kg/s to 0.7 kg/s.

Condenser and Evaporator Water Mass Rate Effect on Performance Coefficient: Fig (16) and (17) respectively show performance coefficient VS water mass rate variation in condenser and evaporator. These figures show that R407C always has less performance coefficient than R22.

Fig (16) shows that by increasing water mass rate in condenser, performance coefficient increases. Difference between performance coefficient of R22 and R407C is 9% to 15% for water mass rate 0.362 kg/s to 0.412 kg/s.

Fig (17) shows that by increasing water mass rate in evaporator, performance coefficient increase. By decreasing water mass rate in evaporator, performance

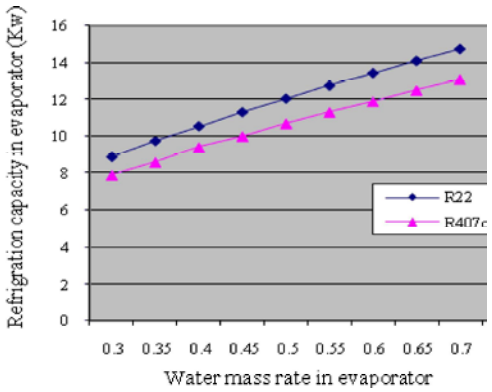

Fig. 15: Evaporator water mass rate effect on evaporator refrigeration capacity

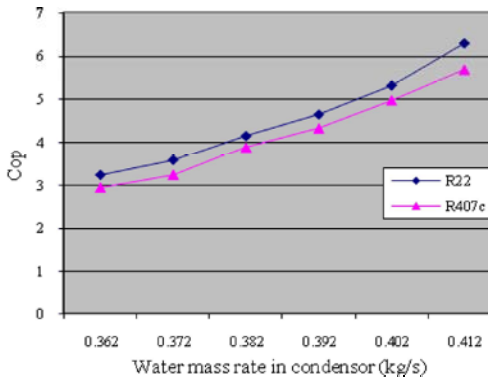

Fig. 16: Condenser water mass rate effect on performance coefficient

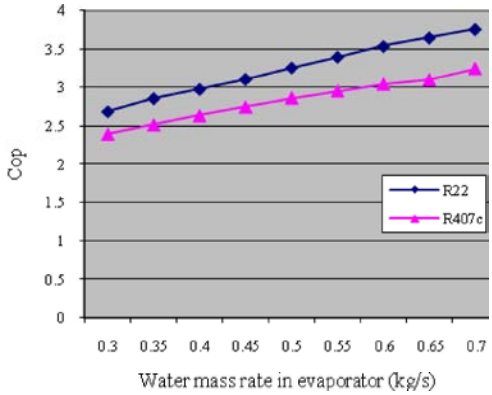

Fig. 16: Evaporator water mass rate effect on performance coefficient

coefficient decreases. Difference between performance coefficient of R22 and R407C is 11% to 14% for water mass rate of 0.3 kg/s to 0.7 kg/s.

CONCLUSION

In this study, performance of compression refrigeration system in off-design point has been studied.

The results show that in various water mass rates for condenser and evaporator, R407C ever has less performance coefficient, refrigeration capacity, refrigerant mass rate and volume efficiency than R22. Results show that by various water mass rate of condenser and evaporator the difference between performance coefficient of R22 and R407C is 9% to 15% for condenser and 11% to 14% for evaporator. The Difference between refrigeration capacities of tow refrigerant is 5% to 9% for condenser and 11% for evaporator. The Difference between refrigeration mass rates is 8% to 12% for condenser and 8% to 9% for evaporator. The Difference between volume efficiency of R22 and R407C is 0.5% to 2% for condenser and 2.5% to 4% for evaporator. By increasing water mass rate in evaporator, evaporator temperature increases.

Therefore, by increasing distillation temperature and decreasing evaporator temperature behavior of R407C approach to R22. Therefore, R407C can be a suitable alternative for replacing with R22 in all of the refrigeration systems with low evaporation temperature.

REFERENCES

1. Francisco J. Uhia, Jame sieres and Antonio Campo, 2007. A general review of the Wilson plot and its modifications to determine convection coefficients in heat exchange devices, Applied Thermal Engineering, pp: 2745-2727.
2. Samuel M. Sami and Daniel E. Desjardins, 2000. Prediction of convective boiling characteristics of alternatives to R-502 inside air/refrigerant enhanced surface tubing, Appl. Thermal Engineering, 20: 579-593.
3. Ru Yang and Fan Pin Chiang, 2002. An experimental heat transfer study for periodically varying-curvature curved-pipe, Int. J. Heat and Mass Transfer, 45: 3199-3204.
4. John W. Rose, Heat-transfer coefficients and Wilson plots, 2004. Accuracy of thermal measurements, Experimental Thermal and Fluid Sci., 28: 77-86.
5. Jose Fernandez-Seara, Francisco J. Uha and Jaime Sieres, 2007. Antonio Campo, A general review of the Wilson plot method and its modifications to determine convection coefficients in heat exchange devices, Appl. Thermal Engineering, 27: 2745-2757.
6. Primal Fernando, Bjorn Palm, Tim Ameel, Per Lundqvist and Eric Granryd, 2009. A minichannel aluminium tube heat exchanger - Part I: Evaluation of single-phase heat transfer coefficients by the Wilson plot method, Int. J. Refrigeration, 31: 669-680.
7. Shokouhmand, H., M.R. Salimpour and M.A. Akhavan-Behabadi, 2008. Experimental investigation of shell and coiled tube heat exchangers using Wilson-plots, Int. Communications in Heat and Mass Transfer, 35: 84-92.
8. Yi Xiaowen and W.L. Lee, 2009. The use of helical heat exchanger for heat recovery domestic water-cooled air-conditioners, Energy Conversion and Management, 50: 240-246.
9. Rani Tusha and P. Balachander, 2008. Numerical Simulation Of fin and tube condenser in a R22 system charged With R407C, J. Scientific and Industrial Res., 67: 209-218.
10. Andries P. Engelbrecht, 2007. Computational Intelligence, Second Edition, 2007, john wiley & Sons, Ltd.
11. Adnan Sozen, Erol Arcakliog lu, Tayfun Menli_k and Mehmet Ozalp, 2008. Determination of thermodynamic properties of an alternative refrigerant (R407c) using artificial neural network, Expert Systems with Applications.
12. Winterton, R.H.S., 1998. Int. J. Heat Mass Transfer, 41: 809.
13. Admiraal D.M. and C.W. Bullard, 1993. Heat Transfer in Refrigrator Condensers and Evaporators,